A New Study of 10 MWe MMLFR Core Designs with considering Natural Circulation

Seungnam Lee and Ser Gi Hong*
Department of Nuclear Engineering, Hanyang University,222 Wangsimni-ro, Seongdong-gu, Seoul, 04763
**Corresponding author: hongsergi@hanyang.ac.kr*

Keywords: MMLFR, ultra-long-life, TRU, natural circulation

1. Introduction

The evolution of nuclear power plants is trending towards Small Modular Reactors (SMRs), with a particular focus on incorporating Generation IV reactor technologies. Our group have investigated a 35 MWt (~ 10 MWe) micro modular lead-cooled fast reactor (MMLFR) utilizing nitride-type fuel [1,2]. This design incorporates Transuranic (TRU) elements from Pressurized Water Reactor (PWR) spent fuel as fuel, aiming to enhance core performance and promote the utilization of nuclear waste.

Natural circulation is also a key consideration in our design, as such systems can significantly improve safety through passive operation compared to forced circulation [3]. We have studied core designs with varying fuel rod lattice configurations: a tight lattice (pitch-to-diameter (p/d) ratio = 1.18) and a loose lattice (p/d ratio = 1.30).

This study examines the neutronic core performance and reactivity coefficients of these designs, as well as their impacts on pressure drop within the reactor system. By analyzing these factors, we aim to optimize the MMLFR design for both neutronic performance and natural circulation.

2. Core Design and Computational Methods

2.1 Core Models

The basic core design started from the MMLFR that our group has been researching [1]. This reactor core utilizes nitride fuel and hexagonal fuel assemblies, with HT-9 steel employed as the cladding and structural materials. To facilitate natural circulation, we modified several core parameters: increasing the pitch-to-diameter (p/d) ratio, reducing the active core height, and increasing the fuel rod diameter to consider cycle length. The design goals for these cores are: 1) achieving a cycle length exceeding 30 years, 2) attaining a burnup greater than 50 MWd/kgHM, which is comparable to that of commercial reactors, 3) ensuring reactivity swings remain below 1 $ for avoiding some Unprotected Transient OverPower (UTOP) accidents [4], and 4) accomplishing negative or small positive (<1 $) coolant void reactivity worth.

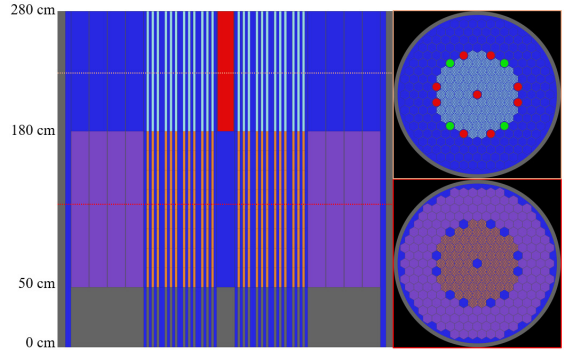

(a) Design A-1

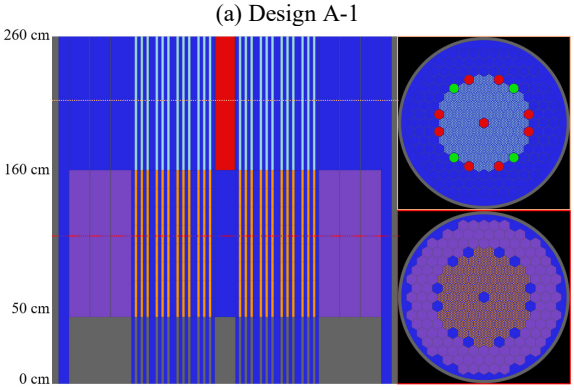

(b) Design B-1

Figure 1. Configurations of the single region cores

Table I: Main design parameters of the cores

Parameters	Design A	Design B
Power (MWt)	35	
Rod diameter (cm)	1.60	2.00
P/D ratio	1.18	1.30
Fuel assembly pitch	11.6983	16.1100
Active core height (cm)	130	110
Average linear power density (W/cm)	101.06	119.44
Average volumetric power density (W/cc)	50.26	38.02
Fuel type	UN (99 wt% ^{15}N)	
Number of fuel assembly	72	
Number of rods in a fuel assembly	37	
Smear density (%)	87	
Cladding thickness (mm)	0.55	0.69
Cladding material	HT-9	
Control rod diameter (cm)	10.6	15.3
Control rod cladding thickness (mm)	1.50	
Number of control rods	13	
Control rod material	40 vol% B_4C + 60 vol% W	
Reflector material	natural Pb	
Barrel thickness (cm)	5	
Barrel material	HT-9	

Figure 1 illustrates two core designs for the MMLFR. Design A features fuel rods with a diameter of 1.6 cm, a

cladding thickness of 0.55 mm, and an active core height of 130 cm. In contrast, Design B incorporates fuel rods with a larger diameter of 2.0 cm, a cladding thickness of 0.69 mm, and a reduced active core height of 110 cm. Nitride-type fuel enriched with 99 wt% ^{15}N was utilized in this study. This specific isotopic composition was chosen to avoid the generation of long-lived radioisotopes through the $^{14}N(n,p)^{14}C$ reaction and to increase cycle length. Table I provides a comprehensive summary of the detailed design parameters for both design cores.

To achieve higher cycle length and burnup, we introduced a two-region core design. TRU are utilized in the inner region. This TRU is derived from spent fuel of commercial PWRs, which has a fuel enrichment of 3.8 wt%, a burnup of 45 MWd/kg, and a cooling time of 15 years.

The TRU is combined with depleted uranium to form ^{depl}U-TRU-N nitride fuel. Figure 2 illustrates configurations for two-region cores. In these configurations, the TRU-based fuel is located in the inner region, arranged in two radial rings and occupying three-quarters of the axial length including the core center.

To enhance gravity-driven insertion of control rods and eliminate control rod ejection accidents, we increased their density by utilizing a mixture of control material and tungsten, rather than conventional B_4C, following the ENHS concept [5]. The control rod assemblies are surrounded by 1.928 mm of HT-9 cladding. For the reflector, we employed lead, which is the same material as the coolant, and encased it in HT-9, same as the control assembly cladding. The entire core is surrounded by a 5 cm thick HT-9 barrel on its periphery.

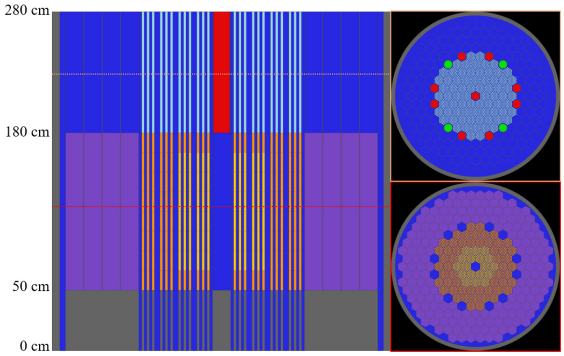

(a) Design A-2

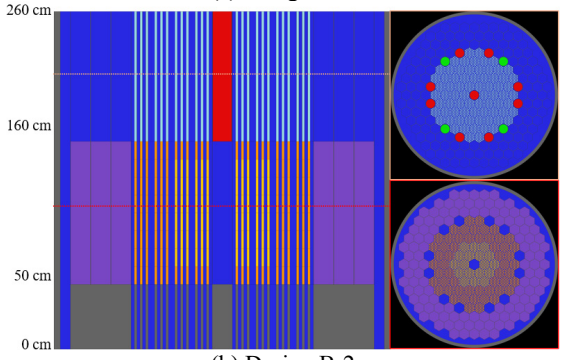

(b) Design B-2

Figure 2. Configurations of the two region cores

2.2 Serpent2

Neutron transport and depletion calculations for full-core 3-D analysis were performed using the Serpent2 code. Serpent2 is a widely recognized Monte Carlo code for reactor burnup calculations, utilizing continuous-energy cross-sections. This code has been under development at VTT Technical Research Centre of Finland since 2004 [6].

A full-core 3-D analysis was conducted, maintaining fuel pin level heterogeneities. The Chebyshev Rational Approximation Method (CRAM) was employed for burnup depletion calculations. Each fuel assembly was discretized into one radial depletion zone and eight axial zones, with depletion time steps set at one-year step. For both neutron transport calculations and depletion analysis, we utilized the ENDF/B-VIII.0 point-wise continuous cross-section library.

The Monte Carlo method for criticality calculations requires an initial set of inactive cycles to allow for fission source convergence, followed by active cycles to collect statistical data. In our analysis, we employed 100 inactive cycles followed by 300 active cycles, with 120,000 neutron histories per depletion step. This approach was used to achieve standard deviations in the effective multiplication factors (k_{eff}) of less than 10 pcm during depletion.

2.3 ORIGEN

The TRU compositions from PWR spent fuel, intended for loading into the inner core, were estimated using the ORIGEN module of the SCALE 6.2 code, developed by Oak Ridge National Laboratory (ORNL) [7]. For this analysis, we employed the cross-section library embedded in the SCALE code utilizing the ARP module. The ARP module facilitates the use of reactor-type cross-section libraries. In this study, we adopted the Westinghouse 14x14 type cross-section library for our calculations.

3. Results

3.1 Single Region Models

LFR aims for long-cycle operation with fuel breeding resulting from the fast spectrum. Figure 3 shows the effective multiplication factors and reactivities for each design. The uranium enrichment was determined to achieve a k_{eff} of 1.004 at the Beginning-of-Cycle (BOC). The End-of-Cycle (EOC) is defined as when k_{eff} falls below 1.0025, considering uncertainty. And the Middle-of-Cycle (MOC) was considered as the middle step between BOC and EOC.

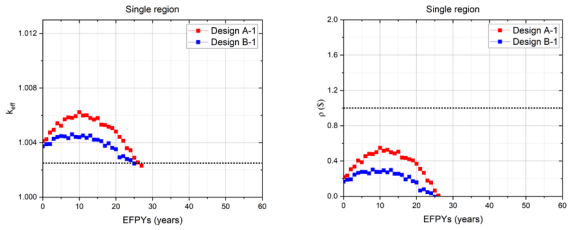

Figure 3. Comparison of the effective multiplication factors and reactivity evolutions of single region designs
(Left: k_{eff} / Right: ρ)

Table II: Comparison of performances of single region designs

Performance	Design A-1	Design B-1
Enrichment (wt%)	12.09	12.23
EFPYs (years)	26	24
Maximum reactivity swing ($)	0.549	0.303
Burnup (MWd/kgHM)	46.83	34.06
3D power peaking factor (BOC/EOC)	1.802 / 1.759	1.798 / 1.766

Table II summarizes the performances of the single region core designs. Design A achieved a cycle length of 26 years with a burnup of 46.83 MWd/kg, while Design B exhibited a cycle length of 24 years with a burnup of 34.06 MWd/kg. The lower burnup of Design B can be attributed to its larger rod diameter, which results in a larger initial uranium mass. The reactivity swing was calculated using Eq. (1). The unit dollar ($) of reactivity is normalized to the effective delayed neutron fraction (β_{eff}) at each depletion step. It is noted that the Design B core has a lower reactivity swing than the Design A one.

$$\rho\ (pcm) = \frac{k_{eff}-1.0025}{k_{eff}*1.0025} * 10^5 \ / \ \rho\ (\$) = \frac{\rho\ (pcm)}{\beta_{eff}\ (pcm)}\ . \qquad (1)$$

3.2 Two Region Models

To enhance core performance, we investigated two-region core models. Our primary objectives were to achieve higher cycle length and burnup by utilizing ^{depl}U-TRU-N fuel in the inner region, utilizing its advantageous breeding characteristics. As illustrated in Figure 3, Design A-2, which incorporates TRU fuel loading, exhibits a significantly extended cycle length due to enhanced breeding capabilities. However, this design encountered a challenge: the reactivity value exceeded the design goal of 1 $. This increase in the dollar value of reactivity can be attributed to two factors. First, there was a higher k_{eff} resulting from increased breeding. Second, the presence of TRU isotopes, which have lower delayed neutron fractions compared to uranium, led to a smaller β_{eff}.

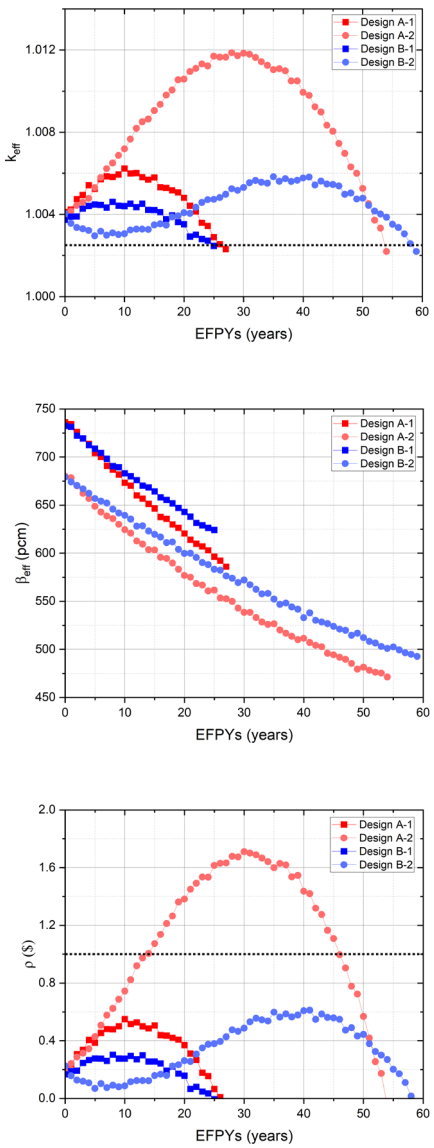

Figure 3. Comparison of the effective multiplication factor and reactivity evolutions of all designs
(Up to Down: k_{eff} / β_{eff} / ρ)

Table IV summarizes the core performance for all core models. The TRU enrichment in the inner region is fixed at 10 wt%, while the uranium enrichment in the outer region is adjusted to achieve an initial k_{eff} = 1.004. The two-region models demonstrate significantly higher cycle lengths and burnups compared to their single-region models. The two-region models (i.e., Design A-2 and Design B-2) attain 53 and 58 years with burnups of 95.46 and 79.01 MWd/kg, respectively.

Furthermore, B-2 exhibits more uniform breeding characteristics than A-2, with its maximum reactivity of 0.612 $ remaining below the 1 $ design goal, thus satisfying the reactivity swing criterion. Additionally, the two-region models generally give the lower 3D power peaking factors compared to the single-region models,

indicating a more uniform power distribution throughout the core.

3.3 Reactivity Feedback Coefficients

Table V summarizes the reactivity feedback coefficients: fuel Doppler effect, radial expansion, fuel axial expansion, coolant void worth, and control rod worth at BOC, MOC, and EOC. All reactivity coefficients, except for the coolant expansion coefficient, are negative. The coolant expansion coefficient, while positive, is almost small.

The void worth in the active core region is negative or slightly positive for the single-region models, but the two-region models exhibit large positive values of approximately 1000 pcm. However, when coolant voiding occurs in both the active core region and upper plenum region, the void worth value decreases significantly. For single-region designs, A-1 and B-1 demonstrate values of -438 and -1282 pcm at BOC, -250 and -1120 pcm at MOC, and -66 and -892 pcm at EOC, respectively. In contrast, two-region designs A-2 and B-2 show values of 546 and -8 pcm at BOC, 531 and 152 pcm at MOC, and 481 and 138 pcm at EOC, respectively. These results indicate that the void worth of two-region models is generally higher than that of single-region models, and that Design B consistently exhibits a lower void worth than Design A. Anyway, the Design A-2 core would have coolant void worth less than 1$ at core cycle if the slightly reduced cycle length is considered.

3.4 Friction Pressure Drop

Natural circulation in a closed circuit is a phenomenon resulting from the density differences in different parts of the medium, caused by thermal imbalance. With heating at the core and cooling at heat exchanger with higher elevation, a favorable density gradient is created, which causes the warmer, less dense fluid to rise, under the action of buoyancy, and cooler, denser fluid to descend [8]. This section examines the pressure drop within the core for each design. Eq. (2) represents the total pressure drop of the reactor system, where the RHS comprises frictional, gravitational, acceleration, and form loss pressure drops, respectively.

$$\Delta P_{tot} = \Delta \mathrm{p}_{\mathrm{fric}} + \Delta \mathrm{p}_{\mathrm{grav}} + \Delta \mathrm{p}_{\mathrm{acc}} + \Delta \mathrm{p}_{\mathrm{form}}. \quad (2)$$

In liquid metal-cooled reactors, the buoyancy effect is the primary driving mechanism of coolant circulation. While a comprehensive analysis would require the consideration of all pressure drop components, this study focuses specifically on the friction pressure drop occurring within the core region but in the future we will consider the other components related to the pressure drops.

The core designs considered in this study incorporate wire-wrapped fuel bundles without duct, a configuration widely adopted in metal-cooled Gen IV reactors due to its superior heat transfer characteristics and lower friction pressure drop. To calculate the friction pressure drop, we employed the simplified Cheng-Todreas correlation [9]. The Chun's research demonstrated that this simplified correlation shows good agreement with experimental values [10].The pressure drop of the fluid is calculated from the following equation:

$$\Delta P = f \frac{L}{D_e} \frac{\rho V^2}{2}. \quad (3)$$

This empirical correlation can be calculated differently depending on whether the Reynolds number is in the laminar region, the turbulent region, or the transient region.

The friction pressure drop in a wire-wrapped fuel bundle can be calculated using the Cheng-Todreas correlation, which is expressed by the following equations:

For laminar region, $\mathrm{Re} < \mathrm{Re_L}$

$$f = C_{fL}/Re, \quad (4\text{-}1)$$

for turbulent region, $\mathrm{Re} > \mathrm{Re_T}$

$$f = C_{fT}/Re, \quad (4\text{-}2)$$

for transition region, $\mathrm{Re_L} < \mathrm{Re} < \mathrm{Re_T}$

$$f = \left(C_{fL}/Re\right)(1-\psi)^{1/3} + \left(C_{fT}/Re^{0.18}\right)\psi^{1/3}, \quad (4\text{-}3)$$

where

$$Re_L = 300\left(10^{1.7(P/D-1.0)}\right), \quad (4\text{-}4)$$

$$Re_T = 10{,}000\left(10^{0.7(P/D-1.0)}\right), \quad (4\text{-}5)$$

$$\psi = \log(Re/Re_L)\ /\log(Re_T/Re_L), \quad (4\text{-}6)$$

$$C_{fL} = (-974.6 + 1612.0(P/D) - 598.5(P/D)^2)\ (H/D)^{0.06-0.085(P/D)}, \quad (4\text{-}7)$$

$$C_{fT} = (0.8063 - 0.9022(\log(H/D)) + 0.3526\ (\log(H/D))^2)\ (P/D)^{9.7}(H/D)^{1.78-2.0(P/D)}. \quad (4\text{-}8)$$

Table III summarizes the calculated friction pressure drop within the core. The core inlet and outlet temperatures were fixed at 400°C and 560°C, respectively. The inlet and outlet coolant velocities were calculated to be compatible with these temperature conditions. Based on these calculations, Design A resulted in a pressure drop of 6.3×10^4 Pa, while Design B exhibited a significantly lower value of 5.8×10^3 Pa, representing nearly lower pressure drop by a factor of 10.

Table III: Comparison of the friction pressure drops in active core

Parameter	Design A	Design B
Active core height (cm)	130	110
Inlet velocity (m/s)	0.408	0.166
Outlet velocity (m/s)	0.416	0.169
Friction pressure drop (Pa)	6.30×10^4	5.81×10^3

From the perspective of friction pressure drop, these results indicate that Design B is easier for natural circulation than Design A.

4. Conclusions

This study presented two core designs for a 35 MW thermal power MMLFR. Compared to the previous study, we increased the p/d ratio and reduced the active core height to better accommodate natural circulation. The two region models incorporating TRU in central region achieved significantly increased cycle lengths and burnups. In particular, the Design A-2 core using thinner fuel rod and smaller p/d ratio showed longer cycle length and higher burnup but the reactivity swing was higher than 1$. On the other hand, the Design B-2 core using thicker fuel rod, higher p/d ratio, and shorter core height showed good core performances such as lower burnup reactivity swing than 1$, longer cycle length than 58 EFPYs, higher discharge burnup than 79 MWd/kg, and smaller coolant void worths less than 1$ under coolant voiding both in active core and upper gas plenum.

Additionally, we evaluated the pressure drop within the core, focusing particularly on the frictional pressure drops, using the simplified Cheng-Todreas correlation for the considered two core designs. From the results, it was shown that estimated Design B which uses thick fuel rod, large p/d ratio, and shorter core height has approximately one-tenth of the friction pressure drop compared to Design A, suggesting its potential to natural circulation.

Acknowledgment

This work is financially supported by the Korea Institute of Energy Technology Evaluation and Planning (KETEP) grant funded by the Ministry of Trade, Industry and Energy (MOTIE) of Republic of Korea (No. RS-2024-00509678) and by the Nuclear Safety Research Program through the Regulatory Research Management Agency for SMRS (RMAS) and the Nuclear Safety and Security Commission (NSSC) of the Republic of Korea (No. 1500-1501-409).

REFERENCES

[1] Y.Y. Cho, S.G. Hong, Ultra Long Cycle MMLFR (Micro Modular Lead-cooled Fast Reactor) Cores using PWR Spent Fuel TRU, Transactions of the Korean Nuclear Society Spring Meeting, Jeju, Korea, May 19-20, 2022.

[2] S. Lee, S.G. Hong, New Design Core Options of Micro-Modular Lead Cooled Fast Reactors (MMLFR) for Facilitating Natural Circulation, PHYSOR 2024, San Francisco, CA, April 21–24, 2024. https://doi.org/10.13182/PHYSOR24-43464

[3] K.H. Ryu, B.M. Ban, T.H. Lee, J. Lee, S.H. Lee, J.H. Cho, S. Ko, J.H. Kim, Natural circulation characteristics under various conditions on heavy liquid metal test loop, International Journal of Thermal Sciences 132 (2018) 316–321. https://doi.org/10.1016/j.ijthermalsci.2018.06.015.

[4] M. Bai, B.A. Lindley, T. Abram, Fuel options for nuclear ship reactors featuring reactivity swing below one dollar, Nuclear Engineering and Design 360 (2020) 110494. https://doi.org/10.1016/j.nucengdes.2019.110494.

[5] S.G. Hong, E. Greenspan, Y.I. Kim, The Encapsulated Nuclear Heat Source (ENHS) Reactor Core Design, Nuclear Technology 149 (2005) 22–48. https://doi.org/10.13182/NT05-A3577.

[6] J. Leppänen, M. Pusa, T. Viitanen, V. Valtavirta, T. Kaltiaisenaho, The Serpent Monte Carlo code: Status, development and applications in 2013, Annals of Nuclear Energy 82 (2015) 142–150. https://doi.org/10.1016/j.anucene.2014.08.024.

[7] B. T. Rearden, R. A. Lefebvre, and M. A. Jessee, SCALE CODE SYSTEM, ORNL/TM-2005/39 Ver 6.2.4, Oak Ridge National Laboratory, 2020.

[8] D.N. Basu, S. Bhattacharyya, P.K. Das, A review of modern advances in analyses and applications of single-phase natural circulation loop in nuclear thermal hydraulics, Nuclear Engineering and Design 280 (2014) 326–348. https://doi.org/10.1016/j.nucengdes.2014.09.011.

[9] S.K. Cheng, N.E. Todreas. Hydrodynamic models and correlations for bare and wire-wrapped hexagonal rod bundles—bundle friction factors, subchannel friction factors and mixing parameters. Nuclear engineering and design 92.2 (1986) 227-251. https://doi.org/10.1016/0029-5493(86)90249-9.

[10] M.H. Chun, K.W. Seo, An experimental study and assessment of existing friction factor correlations for wire-wrapped fuel assemblies, Annals of Nuclear Energy 28 (2001) 1683–1695. https://doi.org/10.1016/S0306-4549(01)00023-8.

Table IV: Comparison of performances of all core designs

Performances	Design A-1	Design A-2	Design B-1	Design B-2
Enrichment (wt%)	12.09	-	12.23	-
inner	-	10	-	10
outer	-	13.89	-	14.07
EFPYs (years)	26	53	24	58
Burnup (MWd/kgHM)	46.83	95.46	34.06	79.01
inner	-	107.24	-	81.50
outer	-	92.74	-	78.44
Maximum reactivity swing ($)	0.549	1.701	0.303	0.612
Average effective delayed neutron fraction (pcm)	660	561	675	576
3D power peaking factor (BOC/EOC)	1.802/1.759	1.622/1.669	1.798/1.766	1.590/1.559

Table V: Comparison of reactivity feedback coefficients of all core designs

Coefficients (BOC/MOC/EOC)	Design A-1	Design A-2	Design B-1	Design B-2
Reactivity coefficients (pcm/K)				
Doppler coefficient	-0.387/-0.326/-0.289	-0.268/-0.332/-0.030	-0.328/-0.496/-0.169	-0.506/-0.534/-0.159
Radial expansion coefficient	-0.478/-0.447/-0.481	-0.491/-0.475/-0.519	-0.426/-0.491/-0.455	-0.445/-0.520/-0.497
Axial expansion coefficient	-0.197/-0.199/-0.202	-0.189/-0.195/-0.203	-0.151/-0.158/-0.159	-0.156/-0.161/-0.164
Coolant expansion coefficient	-0.0003/0.0004/0.0003	0.0009/0.0011/0.0011	-0.0002/-0.0004/0.0003	0.0005/0.0010/0.0013
Coolant void worth (pcm)				
active region	-22.8/140.1/279.7	966.1/871.4/783.1	-85.4/6.9/176.9	1194.7/1169.0/1060.1
active + upper regions	-438.0/-249.7/-65.7	545.8/530.5/481.2	-1281.9/-1119.7/-892.0	-7.9/152.1/138.0
Control rod worth (pcm)				
primary	9875/9639/9505	9464/9009/8873	8387/8318/8193	7762/7694/7645
primary + secondary	11960/11720/11490	11917/11141/10759	9947/9910/9799	9878/9524/9216